JMEPEG (2003) 12:674-686

A Journey With Prasad's Processing Maps

S. Venugopal and P.V. Sivaprasad

(Submitted 15 June 2003; in revised form 10 August 2003)

The constitutive flow behavior of austenitic stainless steel types AISI 304L, 316L, and 304 in the temperature range of 873 K (600 °C) to 1473 K (1200 °C) and strain-rate range of 0.001 s^{-1}-100 s^{-1} has been evaluated with a view to establishing processing-microstructure-property relationships during hot working. The technique adopted for the study of constitutive behavior is through establishing processing maps and instability maps, and interpreting them on the basis of dynamic materials model (DMM). The processing maps for 304L have revealed a domain of dynamic recrystallization (DRX) occurring at 1423 K (1150 °C) at 0.1 s^{-1}, which is the optimum condition for hot working of this material. The processing maps of 304 predict DRX domain at 1373 K (1100 °C) and 0.1 s^{-1}. Stainless steel type 316L undergoes DRX at 1523 K (1250 °C) and 0.05 s^{-1}. At 1173 K (900 °C) and 0.001 s^{-1} this material undergoes dynamic recovery (DRY). In the temperature and strain rate regimes other than DRX and DRY domains, austenitic stainless steels exhibit flow localization. Large-scale experiments using rolling, forging, and extrusion processes were conducted with a view to validating the conclusions arrived at from the processing maps. The "safe" processing regime predicted by processing maps has been further refined using the values of apparent activation energy during deformation. The validity and the merit of this refining procedure have been demonstrated with an example of press forging trials on stainless steel 316L. The usefulness of this approach for manufacturing stainless steel tubes and hot rolled plates has been demonstrated.

Keywords dynamic materials model, dynamic recrystallization, hot working, processing maps, stainless steel

1. Introduction

Austenitic stainless steels are processed mechanically into useful shapes using hot, warm, or cold-forming methods. Cold forming of stainless steel parts can be carried out using lubricants such as chlorinated oil, oxalate soap, methacrylic resin, lime, tallow, borax, fat paste, graphite/MoS_2 in oil, in conventional machines such as forge hammers, rolling mills, presses, and swaggers.[1] Enhancement of strength up to 1500 MPa is reported to have been obtained by cold working and subsequently strain aging the more unstable grades.[2] Warm forging and warm rolling can be carried out in the temperature range 773 K (500 °C) to 1073 K (800 °C) for manufacturing stainless steel components. The room temperature mechanical properties of warm worked stainless steels are better than those of cold-worked stainless steels.[3-5] Hot rolling is carried out on slabs soaked at 1493 K (1220 °C).[6] Hot forging is done with the billet temperature in the range 1173 K (900 °C) to 1473 K (1200 °C) using powdered mica, graphite-oil, and glass as lubricants.[7] Hot extrusion has been done at 1453 K (1180 °C) to 1503 K (1230 °C) using molten glass as a lubricant.[8,9-11] The optimum processing parameters—namely, temperature, strain rate and reduction ratio—followed in the current industrial practice are based on expensive trial and error techniques. These parameters vary from one industry to another and are kept as commercial secret.

The most common problems faced in cold rolling operations on stainless steels are edge cracks, waviness, and small sliver defects.[6] In cold-forged parts, internal cracks are observed, which will affect the performance of the components in service. Hot-worked stainless steels may contain some amount of delta ferrite, which is undesirable for some critical applications, where sigma phase formation is anticipated in service.[12] Moreover, the presence of ferrite (>3%) at room temperature is detrimental to hot workability.[13,14] In hot-forged components non-uniform microstructures and internal cracks have been observed.[15] In hot extrusion, the problems faced are transverse cracks and surface imperfections.

A survey has been carried out on the stainless steels extrusions produced in an industry. Figure 1(a) and 1(b) show typical surface imperfections and transverse cracks respectively, observed in AISI 316L pie extruded at 1443 K (1170 °C) and at a ram speed of 300 mm/s. Malick[16] observed that the transverse cracks are due to the presence of ferrite. Figure 1(c) shows cracks observed on cold pilgered tubes manufactured from the hot extruded pipe with fine (unnoticeable with naked eye) surface imperfections. The rejection rates are as high as 60% in some cases. The rejections are because of the presence of the above defects. These defects can be avoided and the rejection rate can be reduced in industry if the processing parameters are accurately determined and controlled during production. Numerous investigations have been oriented toward the optimization of processing parameters for stainless steels by various investigations either by physical or mathematical modeling.[9,17-21] These studies led to the understanding of the mechanisms of hot deformation. However, it is difficult to use them directly for the optimization of workability. Any scientific methodology explored and employed to optimize the processing parameters to produce defect free components is a significant research contribution to the area of manufacturing engineering. Since the materials used in the construction of nuclear reactors are of special grades and the volume of ma-

S. Venugopal and **P.V. Sivaprasad,** Materials Development Group, Indira Gandhi Centre for Atomic Research, Kalpakkam–603 102, Tamil Nadu, India. Contact e-mail: Venu@igcar.ernet.in.

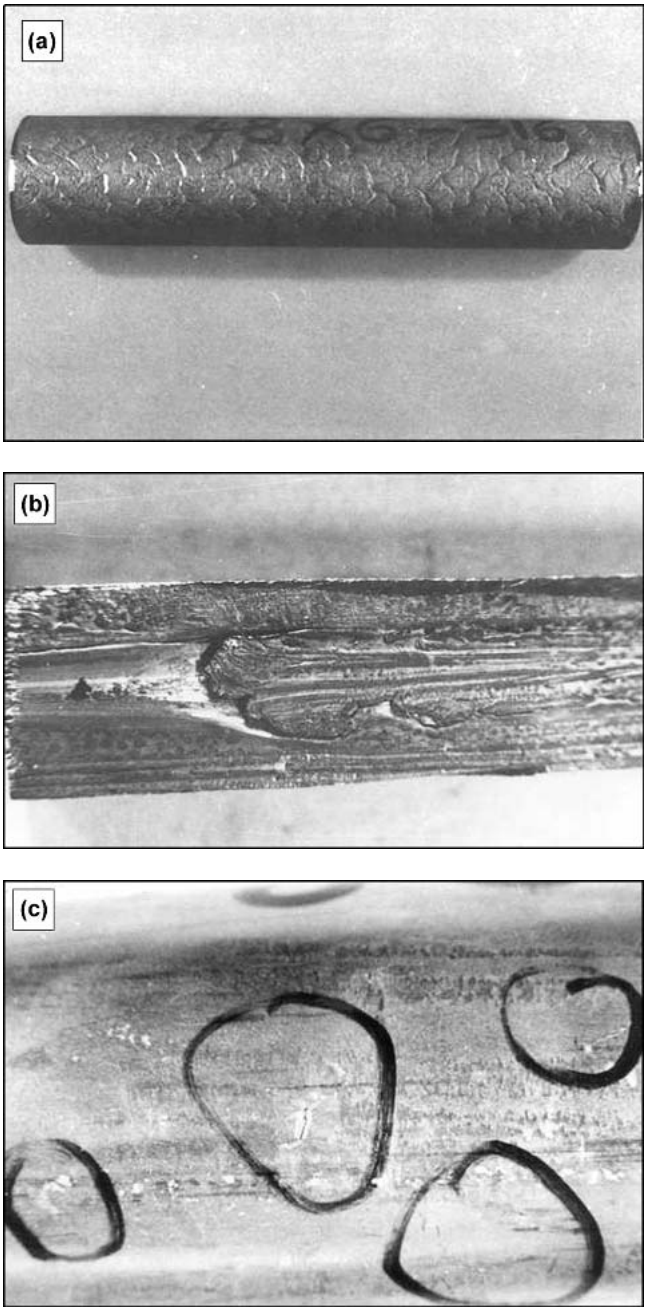

Fig. 1 **(a)** Extruded stainless steel 316L tube with surface defects, **(b)** transverse cracks on the tube, and **(c)** hairline cracks on the pilgered tube

terials are small, the forming technologies should be developed to suit small batch production.

2. Recent Developments in the Design of Metal-Forming Processes

In the recent past, Multidiscipline Process Design and Optimization (MPDO) strategies[22,23] drive part quality, delivery time, and cost. MPDO is a proven strategy for becoming an indispensable supplier for a vendor's customers. It is a set of tools and standards that form an infrastructure to link data and tools from different environments. By means of a MPDO infrastructure based upon commercial software, the design process can be integrated, automated, and accelerated. MPDO helps the design team in (a) creating innovative design alternatives, (b) managing the dynamical and material stability effects in the design of thermomechanical material processes, (c) handling explicitly design objectives and constraints on workpiece materials, processing equipment and tooling, (d) improving product design, (e) reducing the cost and time-to-market, and (f) using simplified models and concepts cost effectively to identify optimal workpiece material trajectories.

The use of the state space (lumped parameter) method[22,23] provides considerable insight into the controllability of metalworking processes. It is a constrained optimization method, where the overall design is specified as constraints and objectives to accommodate multiple physical and economical requirements. This approach identifies optimal workpiece material trajectories that are generally needed for achieving customer product specifications. The ideal forming concepts[23] are based upon the notion that ideal deformation conditions can be visualized and defined for a material and process only if there is a limited set of boundary condition restrictions. These concepts are also based on meaningful material stability conditions and expressing them in the form of nonholonomic (inequality) constraints. The capricious nature of material behavior can be managed by designing the material process to operate primarily in the material stability regions of process parameter space. Most importantly, the analytic microstructure evolution models are only reliable when applied in the stable regions, where microstructure and mechanical property parameter variance is not sensitive to material path trajectory.

Only a near net-shape geometry is possible for several practical reasons: (a) one reason is to keep the residual stress small and to achieve part design allowable; and (b) a second reason is the die life is controlled by the stresses within the die impression and on the die outer shapes. The complexity of the geometry affects both of these process design considerations. For reasons such as these, designers do not usually know *a priori* if some geometric feature is sufficiently significant to rule out the use of simplified process models.

A menu of process analysis methods is available to industrial process design teams to handle almost any material process design problem. It is possible to use ideal design concepts using mesh-based models that have few if any restrictions on geometry. The simplified finite element method (SFEM), for example, corresponds to analysis methods such as the Slab and Upper Bound (UB) methods with respect to computation time and the analysis of a typical step of the forming process. By using appropriate analysis methods, the ideal forming concept is perfect for optimizing different types of material process operations.

3. Optimization of Workability Using the Dynamic Materials Model

Numerous stainless steel components ranging from tiny fasteners and to nuclear reactor vessels are being manufactured by

cold, warm, and hot working techniques for our Prototype Fast Breeder Reactor (PFBR) Program. The 9Cr-1Mo components for steam generators and alloy D9 components for in-core applications are being manufactured for fast reactor program. To achieve the required service properties, it is essential that the microstructural development during hot working be carefully controlled and defects and flow instabilities are avoided. For this purpose, it is desirable that the constitutive flow behavior of the material is adequately characterized in the regimes of temperature and strain rate relevant to hot working. Detailed investigations have been undertaken to evaluate the constitutive flow behavior of austenitic stainless steels, 9Cr-1Mo, and alloy D-9 to establish processing-microstructure relationship during hot and cold working. Stainless steel type AISI 304L has been selected as the basic material for this study since other austenitic stainless steels are compositionally modified versions of this type. The effect of carbon content on hot workability has been studied on commercial 304 and its behavior is compared with that of 304L. Likewise, the effect of molybdenum is evaluated by studying the behavior of 316L. Through studies have also been initiated to evaluate the constitutive flow behavior of indigenously developed 316LN and modified 9Cr-1Mo materials.

The technique adopted for the study of constitutive behavior is through establishing processing and instability maps and interpreting them on the basis of the principles of dynamic materials model.[24] In this model, the efficiency of power dissipation through microstructural changes, given by

$$\eta = 2\,m/(m+1) \qquad \text{(Eq 1)}$$

where m is the strain rate sensitivity, is plotted as a function of temperature and strain rate to obtain a processing map. The different domains exhibited by the map are correlated with specific microstructural processes occurring during hot working. Kumar[25] has shown that flow instability will occur during hot deformation if,

$$\xi(\dot{\varepsilon}) = \{\partial \ln[m/(m+1)]/\partial \ln \dot{\varepsilon}\} + m < 0, \qquad \text{(Eq 2)}$$

where $\dot{\varepsilon}$ is strain rate. The variation of the instability parameter with temperature and strain rate constitutes an instability map, which may be superimposed on the processing map for delineating the regimes of flow instability.

To control the final microstructure of the product, an analytical model for the evolution of microstructure during hot working [in the DRX dynamic recrystallization (1) domain] was obtained. Using the above model, the optimum strain, strain-rate, and temperature trajectories were arrived at to obtain a grain size of 35 μm in an extruded product. Process control parameters, such as ram velocity, die profiles, and billet temperature, which achieve the optimal trajectories, were calculated using a process model. Extrusion trials were conducted at optimal conditions, and good agreement with those predicted in the design stage has been achieved. The results obtained in the case of stainless steel of type AISI 304 material will be discussed in detail.

4. Results and Discussion

Processing maps have been generated for stainless steel types AISI 304, 304L, 304 (as-cast), 316, and 316LN, 9Cr-1Mo, and alloy D9.[26,27] The case of AISI 304L is discussed in detail as an example. The power dissipation map obtained at a strain of 0.5 for stainless steel AISI 304L is shown in Fig. 2(a). The map reveals two distinct favorable domains:

1) A domain occurring in the temperature range of 1273 K (1000 °C) to 1473 K (1200 °C) and strain-rate range of 0.01 s^{-1}, with a peak efficiency of about 33 pct at 1423 K (1150 °C) and 0.1 s^{-1}
2) A domain occurring in the temperature range of 1123 K (850 °C) to 1223 K (950 °C) with the higher strain-rate limit

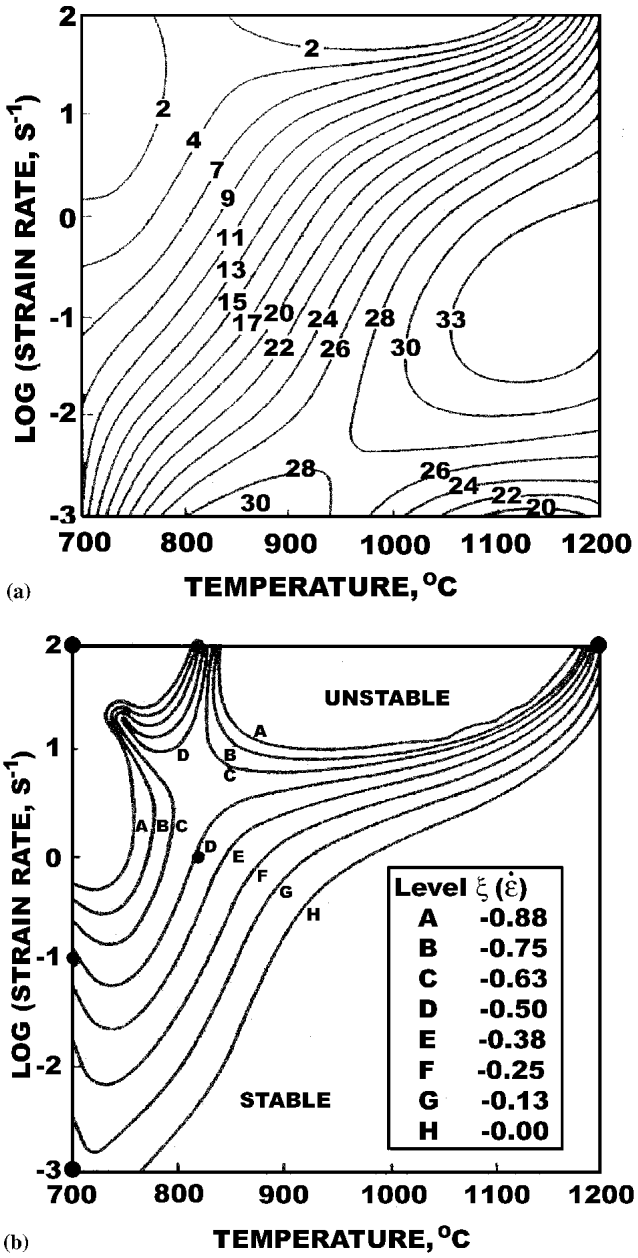

Fig. 2 **(a)** Iso-η contour map (processing map) representing iso-efficiency contours (marked as percent) and **(b)** instability map representing the variation of $\xi(\dot{\varepsilon})$ parameter for stainless steel Type AISI 304L

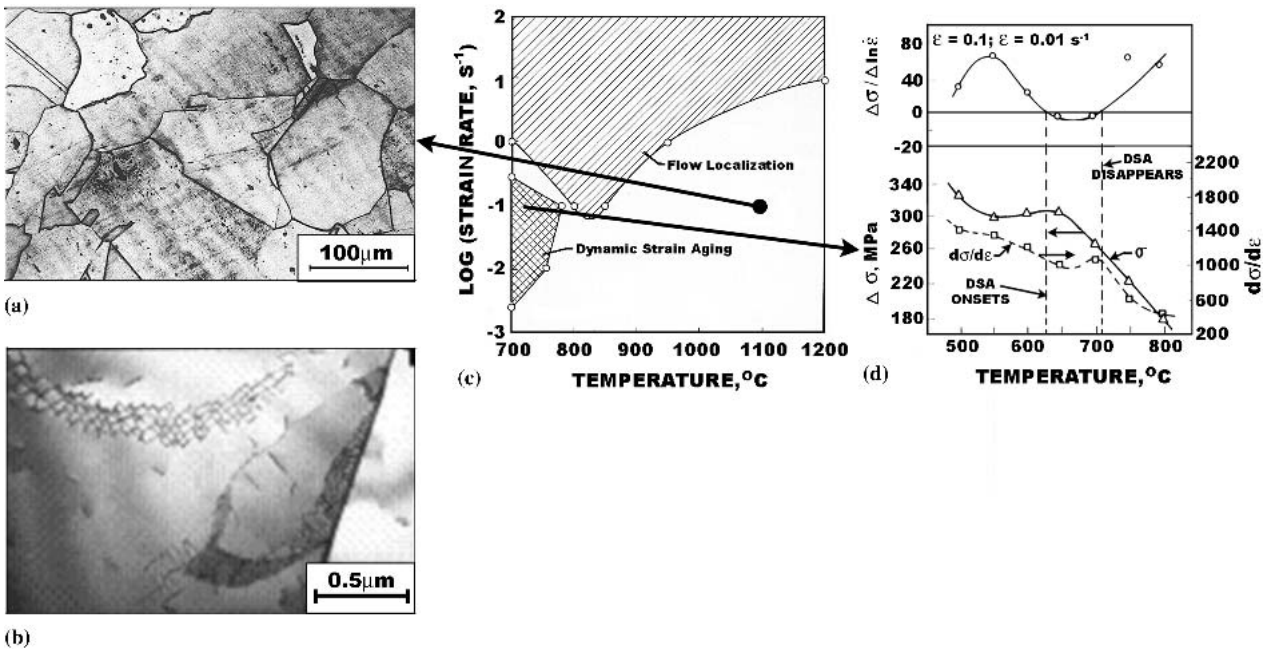

Fig. 3 Typical microstructure of 304L sample deformed at temperature of 1100 °C and strain rate of 0.1 s^{-1} at **(a)** optical level and **(b)** TEM level, **(c)** regions of flow localisation and DSA of 304L in the temperature and strain rate range of 700-1200 °C and 0.001-100 s^{-1}, and **(d)** various manifestations of DSA observed at 0.01 s^{-1} for a true strain of 0.1

at 0.005 s^{-1}, with a peak efficiency of about 30 pct at 1123 K (850 °C) and 0.001 s^{-1}.

The variation of the instability parameter $\xi(\dot{\varepsilon})$ with temperature and strain rate at a strain of 0.5 is shown in Fig. 2(b). According to this criterion the regimes of the map where $\xi(\dot{\varepsilon})$ is negative will represent unstable flow and are bounded by counter H in Fig. 2(b).

4.1 Dynamic Recrystallization Domain

The true stress-true strain curves for 304L at temperatures higher than 1273 K (1000 °C) and strain rates lower than 1 s^{-1} revealed flow softening. The material exhibited flow softening after reaching a peak stress at a critical strain, and at higher strains, a steady-state flow stress was reached. The critical strain decreases with increasing temperature and decreasing strain rate. The values of flow stress corrected for the adiabatic temperature rise are available elsewhere.[26] The analysis on the critical strain for the initiation of DRX suggests that 304L exhibits DRX in the temperature range 1273 K (1000 °C) to 1473 K (1200 °C) and strain rate range of 0.01 s^{-1}-10 s^{-1}. The hot ductility is higher in the regime under consideration and the combination of temperature and strain rate for the ductility peak is 1423 K (1150 °C) and 3 s^{-1}. In the regime under consideration, the hot-worked grain size variation with temperature is sigmoidal. Typical microstructure of the samples deformed in this region is given in Fig. 3(a), which exhibits the features of DRX such as curved grain boundaries. The subcells are clearly seen in the microstructure of the sample deformed at 1373 K (1100 °C) and 0.1 s^{-1} (Fig. 3b). The above results have confirmed that the material exhibits DRX in the regime under consideration. The process parameters for the optimum workability in 304L stainless steel are 1423 K (1150 °C) and 0.1 s^{-1}, and the temperature and strain rate ranges for obtaining DRX microstructure are 1273 K (1000 °C) to 1473 K (1200 °C) and 0.01 to 10 s^{-1}, respectively. The analysis on the flow curves and microstructural examination indicate that 304L undergoes dynamic recovery (DRY) at 1173 K (900 °C) and 0.001 s^{-1}.[26]

4.2 Flow Localization and Dynamic Strain Ageing Regions

The criterion developed by Semiatin and Lahoti[29] for predicting flow localization has been examined using the present data. According to this criterion, instability will occur if,

$$(1/\dot{\varepsilon})\,(d\dot{\varepsilon}/d\varepsilon) = -(\gamma/\sigma m) > 5 \qquad \text{(Eq 3)}$$

where, ε = strain, γ = work hardening coefficient, and σ = flow stress. The region of flow localization, per Eq 3, is shown in Fig. 3(c). The various manifestations of DSA, such as (a) hump in flow stress versus temperature dependence, (b) negative strain rate sensitivity, and (c) hump in work hardening rate vs. temperature relation[30] have all been observed in the present case. Typical of such behavior is given in Fig. 3(d). The region of DSA is marked in Fig. 3(c).

4.3 Industrial Validation

To substantiate the above predictions of microstructural development during processing, validation experiments such as press forging, hammer forging, rolling, and extrusion, at industrial scale have been carried out. The conditions under which tests were conducted are marked in Fig. 4(a). The forming operations were conducted at different temperatures and the

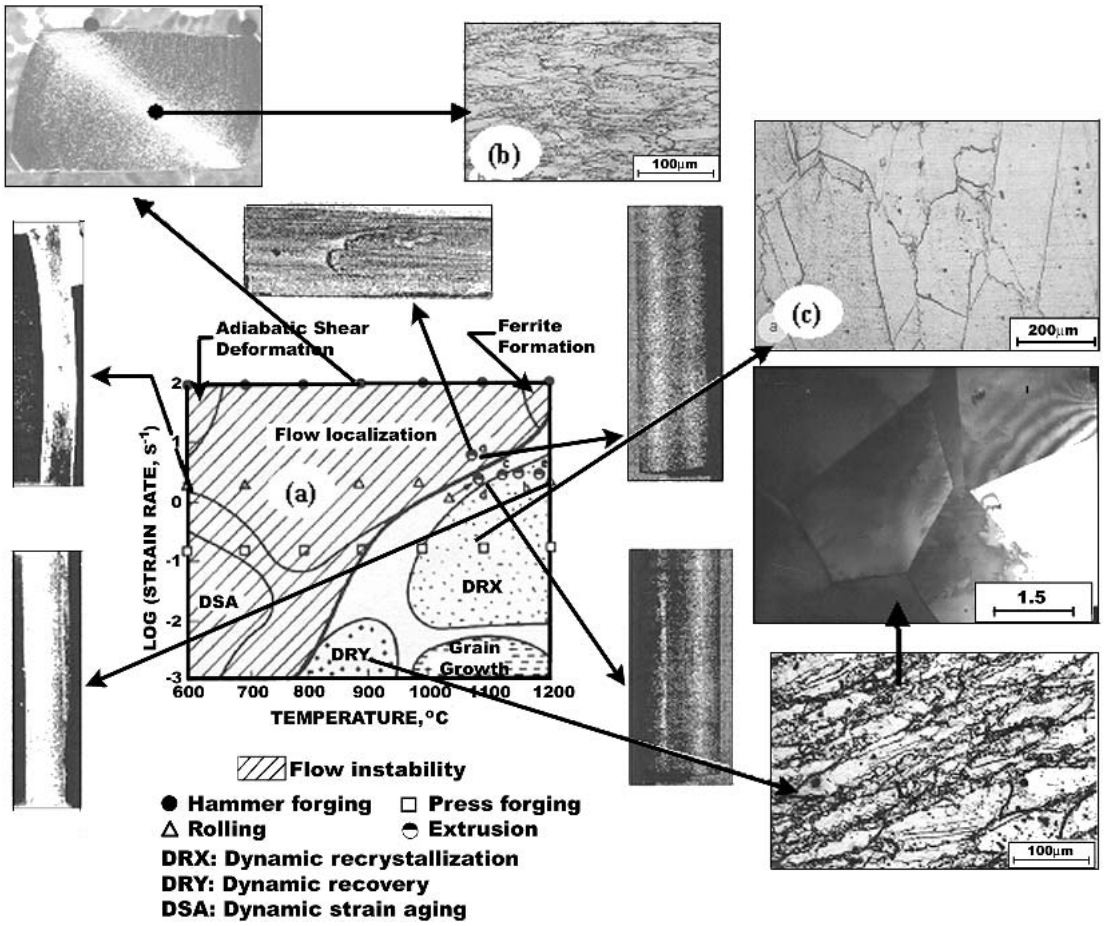

Fig. 4 **(a)** Map representing the domain of various processes for 304L; the condition under which industrial validation tests were conducted are marked. **(b)** Microstructure of the hammer deformed at 800 °C and 100 s^{-1} and **(c)** microstructure of the sample press forged at 1200 °C and 0.15 s^{-1}. The photographs of the products obtained at various regions are also inserted. The macroscopic defects observed on the products are also corroborated well with the findings of the map.

microstructures were studied and correlated with the structures evolved during hot compression tests. The results have shown that excellent correlation exists between the regimes exhibited by the map (Fig. 2) and the product microstructures. For example, the microstructure of 304L product forged at 1473 K (1200 °C) and at 0.15 s^{-1} reveals the features of DRX (Fig. 4c) whereas the product forged at 1073 K (800 °C) and at 100 s^{-1} exhibits features of flow localization (Fig. 4b).

4.4 Processing Maps for 304, 316L, and Alloy D-9

The processing maps of 304 and 316L are given in Fig. 5. In the 304 material, both DRX and DRY have merged and the temperature and strain rate at which DRX and DRY onset is lowered about 50 K (50 °C) and one order of magnitude respectively, from those of 304L. This feature can be explained as follows: in stainless steel the DRX process is nucleation-controlled. In nucleation controlled DRX process, a certain critical strain corresponding to a critical dislocation density is required for generating nuclei for grain boundary migration. The critical strain is therefore thermally activated since it depends on the rate of recovery. Since DRX in 304 is controlled by nucleation, the presence of carbon interstitial will pin the dislocations and reduce the dislocation segment length. Thus, to obtain a required nucleation rate, lower strain rates are sufficient. The decrease in the DRX temperature may be attributed to a decrease in the activation energy for diffusion caused by the formation of vacancy-interstitial pairs.

The onset of DRX in stainless steel type AISI 316L is at temperature of about 100 K (100 °C) higher and at lower strain rates (less than one order) than in 304L. It is well known that molybdenum addition causes high temperature strengthening in 316L stainless steel. In view of this considerable back stress is developed in 316L in comparison with 304L and higher temperature would be required to cause climb in the presence of the large back stress. Since the DRX process is controlled by thermal climb, the DRX temperature in type 316L would be higher than that in 304L. The slight decrease in the DRX strain rate may be attributed to a reduced link length of dislocations and a higher rate of dislocation generation in molybdenum-containing solid solution.

The optimum processing parameters for stainless steel types AISI 304L, 304, 316L, and 304 (as-cast) materials, corresponding to the peak efficiency of the DRX domain are given in

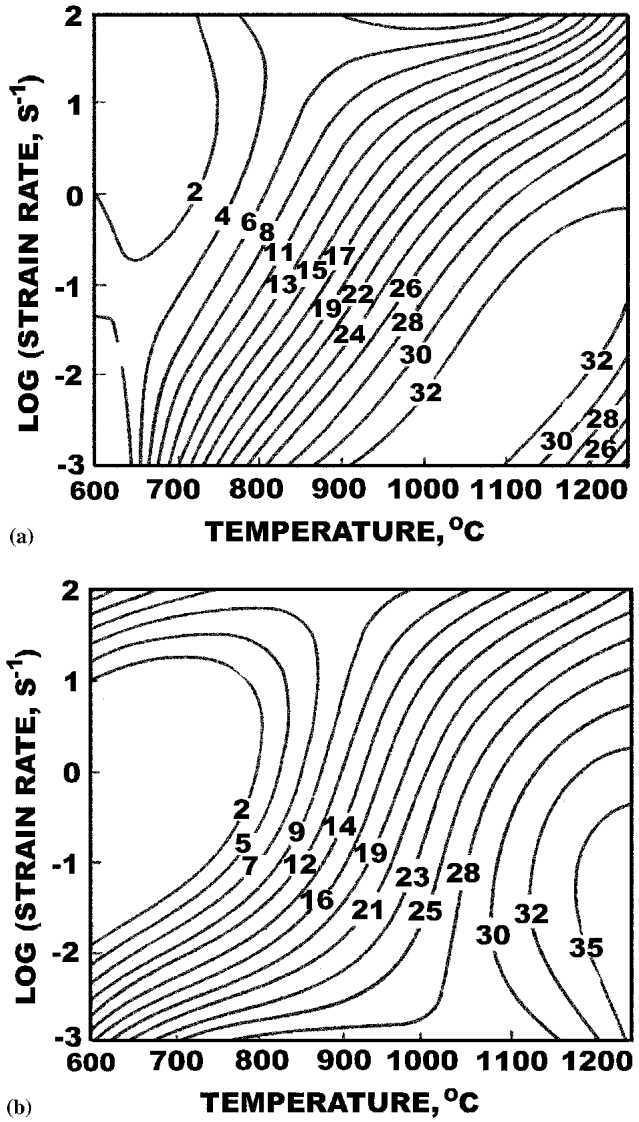

Fig. 5 Processing maps representing iso-efficiency contours (marked as percent) for **(a)** 304 and **(b)** 316L

Table 1. The instability maps for stainless steel types AISI 304L, 316L, 304, and 304 (as cast) has been generated in the temperature range 293 K (20 °C) to 873 K (600 °C) corresponding to the cold and warm working regions. A typical instability map of 304L in the cold and warm working region is given in Fig. 6. A typical consolidated processing and instability map for 316L in the temperature range 293 K (20 °C) to 1523 K (1250 °C) covering cold, warm, and hot working regions is given in Fig. 7. Austenitic stainless steels have exhibited the flow instabilities at lower temperatures below 873 K (600 °C). The general manifestations and regimes are given in Table 2. The three major manifestations of flow localization are (a) martensite formation, (b) dynamic strain aging, and (c) adiabatic shear deformation. Since these regimes introduce inhomogeneous deformation, these are to be avoided during processing.

The processing maps for alloy D-9 is presented in Fig. 8. These maps were characterized through detailed microstructural investigations. The optimum parameters predicted by these maps are 1423 K (1150 °C) to 1523 K (1250 °C) and 0.001-2 s^{-1}. These maps were also validated through press forging, hammer forging, and rolling trails carried out at industrial scale. The development of processing maps for indigenously developed stainless steel type AISI 316LN and Modified 9Cr-1Mo are in progress.

The usefulness of these maps for controlling the industrial processes such as press forging, extrusion, and hammer forging, through detailed experimental investigations carried out at actual industrial process conditions. The finding of these maps have been applied for regular industrial production of seamless stainless steel tubes by hot extrusion. The Nuclear Fuel Complex, Department of Atomic Energy, is following the processing parameters recommended by these maps for the extrusion of stainless steels. The lower ram speed during the initial upsetting and extrusion has improved the yield. The application of the findings of these processing maps has resulted in lower rejection rates (less than 2%) and higher yields in the production of nuclear-grade stainless steel tubes.

5. Refinement of Optimal Window for Processing

The optimal domains predicted by the above approach are wider. In practice, in this wider domain it is very difficult to control the microstructure of the product. Hence some refining procedure is to be established for the precise control of the microstructure during working. Malas and Seetharaman[31] proposed stability criteria based on the DMM. According to them the optimal processing windows for safe working are

$$0 < m \leq 1 \quad \text{(Eq 4)}$$

$$\dot{m} < 0, \quad \text{(Eq 5)}$$

$$s \geq 1 \quad \text{(Eq 6)}$$

$$\dot{s} < 0. \quad \text{(Eq 7)}$$

Where, $\dot{m} = \partial m/\partial \ln\dot{\varepsilon}$, $s = \partial \log\sigma/\partial(1/T)$ and $\dot{s} = \partial s/\partial \log \dot{\varepsilon}$ and T = temperature.

The apparent activation energy $Q = sRT/m$ = Constant, where R = gas constant.

In this methodology the reasonable "safe" processing range corresponds to the processing condition where a desirable and fairly constant value of activation energy is operative. These criteria can be used to refine the safe processing window to achieve better microstructural control during safe processing. The values of m, $\dot{m}$, s, $\dot{s}$, and Q have been calculated and contour maps have been generated for stainless steel type 316L. A typical contour map of the above parameters at a strain of 0.5 is given in Fig. 9. The stable domain, where Q = constant is marked in the figure, which is a refined window for processing.

To substantiate the preciseness of the refining methodology (Fig. 9) press forging tests at industrial scale were carried out on SS 316L in the temperature range 1173 K (900 °C) to 1473 K (1200 °C). The grain size and the room temperature mechanical properties of the forged products were evaluated. The measured grain size as a function of forging temperature is

Table 1 Optimal Parameters for Hot Working of Austenitic Stainless Steels

Material	Optimum Conditions for Working (DRX)	Peak Efficiency for DRX, %	DRX Domain	
			Strain Rate, s^{-1}	Temperature, °C
304L	1150 °C and 0.1 s^{-1}	33	0.01	950-1250
			0.1	1095-1250
			1.0	1050-1250
304	1100 °C and 0.01 s^{-1}	32	0.001	905-1250
			0.01	1000-1250
			0.1	1050-1250
			1.0	1250
304 (as-cast)	1250 °C and 0.001 s^{-1}	40	0.001	1080-1250
			0.01	1090-1250
			0.1	1100-1250
			1.0	1150-1250
316L	1250 °C and 0.05 s^{-1}	42	0.001	1150-1250
			0.01	1080-1250
			0.1	1090-1250
			1.0	1110-1250

given in Fig. 9(b). Figure 9(b) shows that the variance in the grain size of the samples deformed in the stable domain is small. The above feature implies that a small variation in temperature will not cause a change in grain size in the product. Hence, the control of microstructure in the product is precise if the material is processed in the stable regime. The values of ultimate tensile strength (UTS) of the forged products as a function of forging temperature are given in Fig. 9(c). Figure 9(c) shows that the variance in UTS values is very less in the products forged in the stable region where as the scatter is large in the products forged in the unstable regions. The same feature is observed in the values of yield strength (YS) and ductility. When the material is processed within the stable region, metallurgical and mechanical properties have low sensitivity to small variations in external stimuli, and these properties are not sensitive to the path.[32] It is not sensitive to path because the process is operating in an extremum (a region of low and nearly constant activation energy). In the unstable regions, an infinite number of paths can exist, which are sensitive to small variations in external stimuli such as temperature and strain-rate fluctuations.

6. Trajectory Optimization

6.1 Methodology

A new strategy for systematically calculating near-optimal control parameters for the hot deformation process has been proposed for microstructural control.[33] This approach is based on the optimal control theory[34] and involves developing state-space models from available material behavior and hot deformation process models. The control system design consists of two basic stages, and analysis and optimization are critical in both stages. In the first stage, the kinetics of certain dynamic microstructural behavior and intrinsic hot workability of the material are used, along with an approximately chosen optimality criterion, to calculate optimum strain [$\varepsilon(t)$], strain-rate [$\dot{\varepsilon}(t)$], and temperature [$T(t)$] trajectories for processing. A suitable process simulation model is then used in the second stage to calculate process control parameters, such as ram velocity, die profiles, and billet temperature, which approximately achieve the strain, strain-rate, and temperature trajectories calculated in the first stage. This process design approach treats the deforming material as a dynamic system and involves developing state-space models from available material behavior and hot deformation process models. The design approach requires three basic components for defining and setting up the optimisation problem: (a) a dynamic system model, (b) physical constraints, and (c) an optimality criterion. The system models of interest are material behavior and deformation process models. Constraints include the hot workability of the work-piece and the limitations of the forming equipment. Optimality criteria could be related to achieving a particular final microstructure (grain size), regulating temperature, and/or maximizing deformation speeds.

Figure 10 describes the steps involved in the proposed new approach.[33] The microstructure development optimization determines optimal trajectories of strain, strain rate, and temperature. From these optimal trajectories, the process optimisation stage determines optimal process control parameters, namely the die shape, the ram velocity profile, and billet temperature. Goals of the first stage are to achieve enhanced workability and prescribed microstructural parameters. In the second stage, a primary goal is to achieve the thermomechanical conditions obtained from stage one for predetermined regions of the deforming work-piece. In the first stage, models of material behavior that describe the kinetics of primary metallurgical mechanisms such as dynamic recovery, dynamic recrystallization, and grain growth during hot working are required for analysis and optimization of material system dynamics. These mechanisms have been studied extensively, and relationships for describing particular microstructural processes have been developed for a variety of materials.[19] The objective is to define the acceptable ranges of temperature and strain rate over which the material exhibits a "safe" processing window. The "safe" processing window may be identified using any of the proven methodologies.[24,30]

An extrusion process has been designed using the new two-

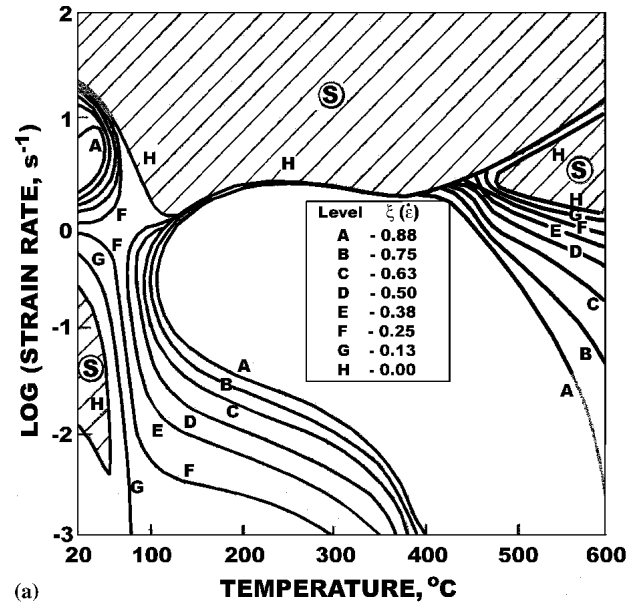

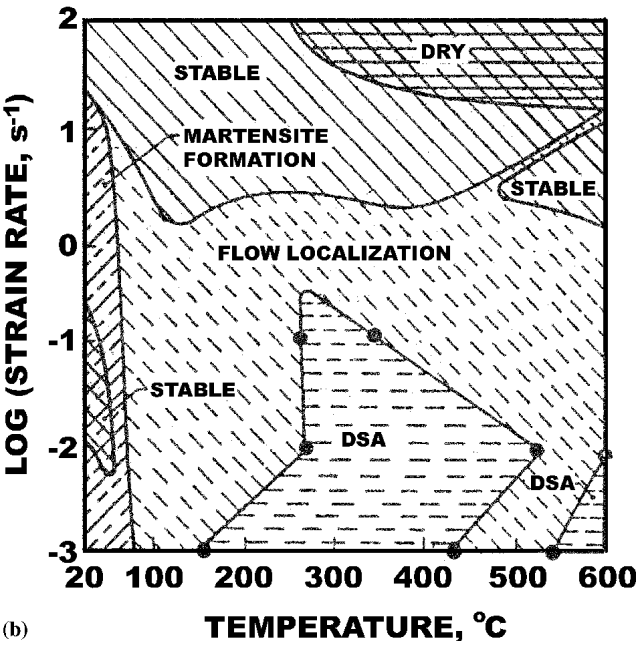

Fig. 6 **(a)** Instability map for 304 stainless steel at a strain of 0.3 representing the variation of $\xi(\dot{\varepsilon})$ parameter. The instability is predicted within H $\xi(\dot{\varepsilon})$ becomes negative. **(b)** Schematic representation of the regions of various processes for 304 (key to Fig. 6a)

stage methodology for stainless steel, type AISI 304L to obtain a desired grain size at 35 μm in the product. To validate the usefulness of the two-stage methodology, extrusion trials were conducted at optimal conditions.

6.2 Generation of a Model for Evolution of Microstructure

The two-stage (Fig. 10) approach is applied for controlling microstructure (in the present case, grain size) during hot extrusion of stainless steel type AISI 304L. The optimum ram

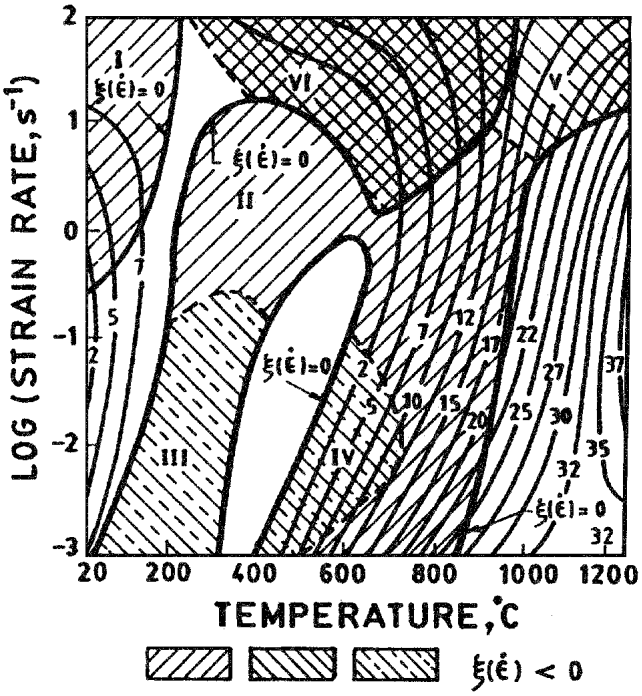

Fig. 7 Contour maps representing iso-efficiency contours (marked as percent) at a strain of 0.5 for 316L; the instability map is superimposed on the processing map and the instability regimes are hatched.

velocity and die profile for extruding 304L to obtain a final grain size of 35 μm have been determined using the above two-stage approach. An empirical model for the DRX process in 304L has been developed for this purpose in the temperature range of 1223 K (950 °C) to 1523 K (1250 °C) and strain rate range of 0.1-20 s^{-1}, which are normal parameters for an extrusion process. Compression tests were performed on 304L in the above temperature and strain rate ranges to generate data for the model. The effects of strain, strain rate and temperature on microstructural evolution of this material during hot working are:

volume fraction recrystallized

$$\chi = 1 - \exp\left[\ln(2)\left(\frac{\varepsilon - \varepsilon_c}{\varepsilon_{0.5}}\right)^2\right] \quad \text{(Eq 8)}$$

critical strain,

$$\varepsilon_c = 5.32 \times 10^{-4} e^{8700/T} \quad \text{(Eq 9)}$$

plastic strain for 50% vol. Recrystallization,

$$\varepsilon_{0.5} = 1.264 \times 10^{-5} d_0^{0.31} \varepsilon^{0.05} e^{6000/T} \quad \text{(Eq 10)}$$

and average recrystallized grain size,

$$d = 20\,560\dot{\varepsilon}^{-0.3} e^{-0.25\left(\frac{Q}{RT}\right)} \quad \text{(Eq 11)}$$

Table 2 Regimes to be Avoided During Cold and Warm Working of Austenitic Stainless Steels

Material	Strain Rate, s^{-1}	Martensite Formation	Temperature, °C		
			Flow Localization	Dynamic Strain Aging	Adiabatic Shear Deformation
304L	0.001	20-80	20-550; 605-760	100-550	…
	0.01	20-40	20-575; 590-890	60-475; 680-760	…
	0.1	…	200-500; 570-940	375-525; 650-800	…
	1.0	…	550-1030	…	…
	10.0	…	600-1180	…	400-600
	100.0	…	600-1200	…	250-600
304	0.001	20-80	20-800	157-450; 550-645	…
	0.01	20-60	20-860	265-535; 600-700	…
	0.1	20-45	20-900	265-345; 650-675	…
	1.0	20-30	20-1000	495-520	…
	10.0	20	20-40; 700-1200	…	…
	100.0	…	875-1250	…	…
304 (as-cast)	0.001	20-40	20-800	160-260; 370-550	…
	0.01	20-30	20-850	60-250; 520-580	…
	0.1	…	350-920	280-370; 440-680	…
	1.0	…	370-1000	…	…
	10.0	…	20-330; 390-500; 480-1100	…	…
	100.0	…	900-1150	…	…
316L	0.001	…	40-300; 400-850	310-510	…
	0.01	…	105-300; 410-905	145-305; 465-700	…
	0.1	…	125-375; 525-930	295-450; 600-620	…
	1.0	…	20-105; 150-960	…	…
	10.0	…	20-80; 295-305; 595-1100	…	400-900
	100.0	…	900-1250	…	200-850

where d_0 = initial grain diameter, ε = strain, T = temperature in K, d = grain diameter μm, Q = 310 kJ/mol, and R = 8.314 × 10^{-3} kJ/molK. Using the above model and flow stress data (for estimating the rate of change of temperature due to deformation) the state-space model for microstructural evolution has been generated.

6.3 Optimization of the Microstructural Trajectories

In the present case a tube extrusion with outer diameter from 137 mm and inner diameter of 40 mm to tube diameter of 48 mm with 6 mm wall thickness (true strain = 3.46) will be considered. The desired final grain size in the product is 35 μm. For the above case, the following optimality criterion was chosen:

$$J = 10[\varepsilon(t_f - 3.46]^2 + \int_0^{tf} (\mathrm{d}(t) - 35]^2 \mathrm{d}t, \qquad \text{(Eq 12)}$$

where a desired final strain of 3.46, with a weight factor of 10, and a desired grain size of 35 μm were specified. The optimal strain, strain rate, and temperature trajectories were obtained using the above criteria and microstructural model. The optimal strain, strain rate. and temperature trajectories are given in Fig. 11(a).

6.4 Optimization of the Process Parameters

Using the following relationships (Eq 13 and 14), the shape of the extrusion die for extruding the material has been obtained:

$$V_{\mathrm{ram}} = L \Big/ \int_{t=0}^{t_f} e^{\varepsilon(t)} \mathrm{d}t \qquad \text{(Eq 13)}$$

$$r(t) = r_0 e^{-\varepsilon(t)/2}, \qquad y(t) = V_{\mathrm{ram}} \int_0^t e^{\varepsilon(t)} \mathrm{d}t, \qquad \text{(Eq 14)}$$

where r_0 is the die entrance radius (equal to the billet radius), L is the die length, and $\varepsilon(t)$ is the required strain trajectory, t is the time interval, V_{ram} is the ram velocity, r is the die radius, and y is the axial distance (die throat length). Figure 11(b) gives the optimum die profile for achieving a final grain size of 35 μm obtained by using this approach. The optimum ram velocity for achieving the above grain size is found to be 160 mm/s when billet temperature is 1353 K (1080 °C).

6.5 Experimental Verification

The design methodology was verified in an industrial environment by means of detailed extrusion experiments with the die having the optimal profile, obtained in this investigation. The extrusion test was performed at optimal conditions of temperature and ram velocity in a horizontal extrusion press of 3 780 ton capacity available at Nuclear Fuels Complex, Hyderabad, India. The billet material was AISI 304L. The outer diameter, inner diameter, and length of the billet were 137, 48, and 500 mm, respectively. The final outer diameter of the tube was 48 mm and wall thickness 6 mm. The ambient temperature of the die, container and follower block was 623 K (350 °C), and soak temperature of the billet was 1353 K (1080 °C). Molten glass was used as lubricant during extrusion. The

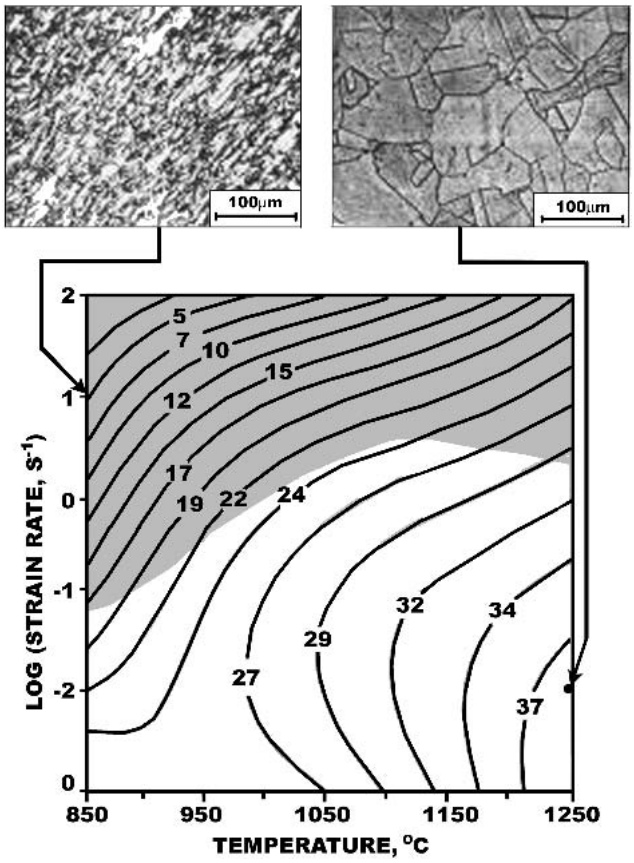

Fig. 8 Processing maps representing iso-efficiency contours (marked as percent) for Alloy D-9

extruded tube was ejected into a water tank immediately after the completion of the extrusion. The extruded piece was cut along its longitudinal axis, polished and etched for microstructural investigation. Microstructural examination carried out along the entire length of the tube revealed that there is no variation in microstructure along the length. Grain size measurements were done using the Hyen intercept method.[35] Histograms were made to find the grain size distribution and the average grain diameter. The measured average grain size was 38 μm, which is close to the designed value.

7. Directions for Future Research

7.1 Development of Dynamical Models

Manufacturing processes can be mathematically modeled as nonlinear dynamical systems using a state-variable formulation, i.e., a system of coupled, first-order non-linear differential equations. The important point concerning dynamical models is that they are valid for a broad range of control signals, unlike algebraic models, which are only valid for a particular class of process controls, such as constant temperature and strain-rate. The use of dynamical models provides greater predictive capability over algebraic models and more degrees of freedom in the time domain for optimal process design. Dynamical models for the material behavior will be generated for 316LN, modified 9Cr-1Mo material, and alloy D-9. Models for various subsystems will also be developed.

7.2 Shape Change Mapping

The goal of achieving more efficient material flow and better control of the spatial distribution of microstructure can be achieved using state space material process models and geometry mapping relationships between starting and finished shapes.[22] A new kind of process model is emerging that is based predominantly on ideal forming concepts and geometrical mapping relationships between the initial and final states.[22] In this approach, a strong emphasis is placed on geometry mapping and the use of simplified models to predict key process parameters.

7.3 Process Control Using Intelligent Control Techniques

The parameters such as temperature of the billet, strain experienced by the billet, and speed of the press slide can easily be measured and controlled effectively during the process. The microstructural state of the billet can be assessed through ultrasonic sensors. The microstructural state of the billet can also be determined indirectly from the values of strain, strain rate, and temperature using the models describing the evolution of microstructure during working. The online determination of grain size during rolling has been attempted and proved to be successful. The important phenomena such as deformation, cracking, lubricant break down, material flow in the die-cavity, and die-closure can be monitored by using the acoustic emission (AE) technique.[38] The authors have carried out some preliminary investigations to examine the feasibility of using AE technique for monitoring forging operation. The authors have predicted AE using simulation technique and compared with that of the experimental investigations. Figure 12 indicates that the predictions based on simulation studies are corroborated well with that of the experimental results.[36] Figure 13 shows the AE recorded at varied friction conditions during open-die forging. Hence, by monitoring of the process one can predict the quality of the parts during forging and apply corrective action during the operation if the quality of the product is not meeting the specification.

An intelligent forging system consisting of a built-in knowledge base system for the design and control of metal forging operation, monitoring tools for the measurement of billet temperature, ram velocity, deformation ratio, friction, to assess the cracking and die fill, and enhanced visualization features, as shown in Fig. 14, has been proposed by Malas[37] to be developed for the design and control of metal forming processes. This system should be capable of predicting the microstructural state, macroscopic features (i.e., dimensions of the deforming billet, surface finish, spring back, etc.) of the billet at various locations using appropriate models during formation and adjusting the process parameters with controllers to correct the deviations if any.

8. Summary

The constitutive flow behavior of stainless steels type AISI 304L, 316L, 304, and 304 (as-cast) and alloy D-9 was studied

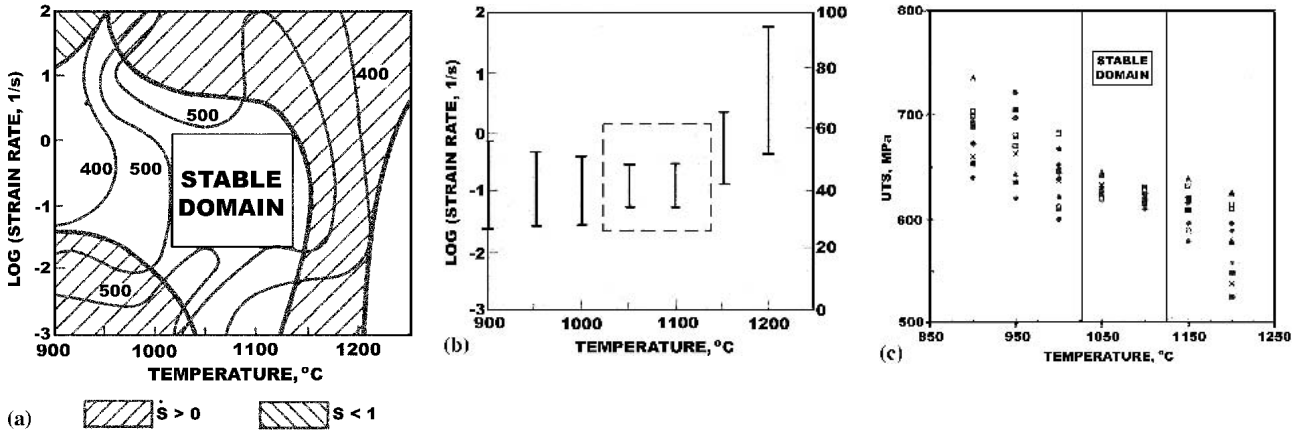

Fig. 9 **(a)** DMM stability map for stainless steel 316L; the values of activation energy are represented as contours in kJ/mol. Variation of **(b)** the grain size and **(c)** UTS of the forged products of 316L as a function of forging temperature is superimposed on the DMM stability map; the products were forged at 0.15 s^{-1}.

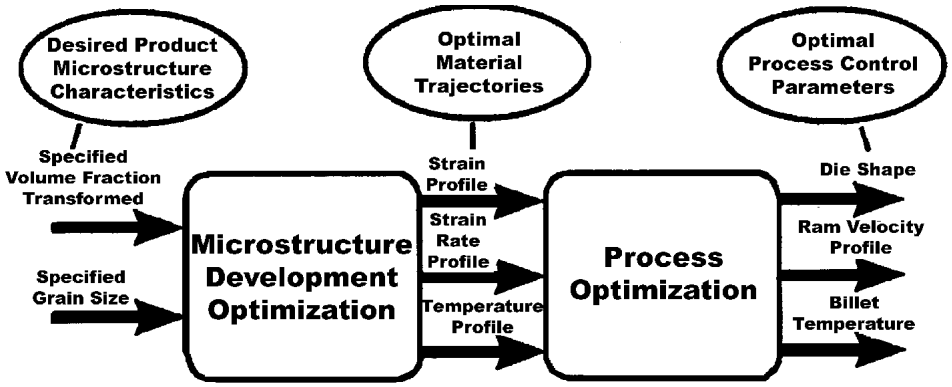

Fig. 10 Schematic of the two-stage approach[33]

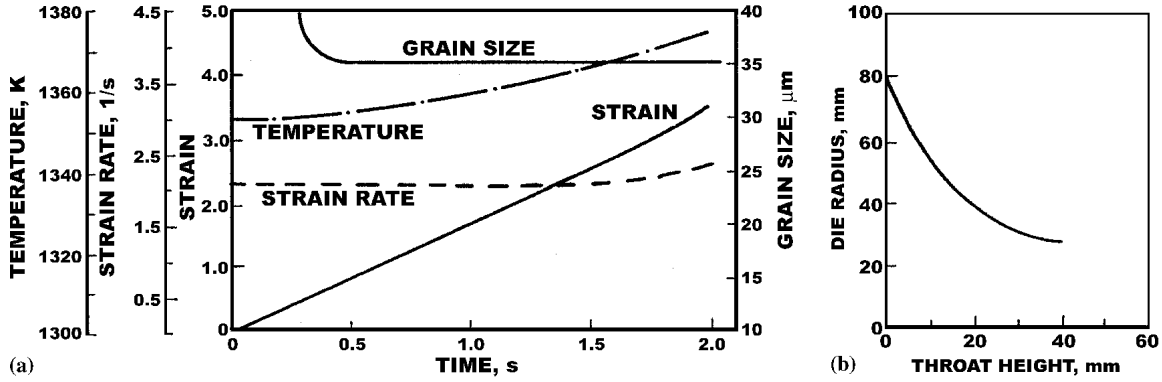

Fig. 11 **(a)** Trajectories of strain, strain rate, temperature, and grain size, **(b)** and optimal die profile for achieving the desired final grain size of 35 μm

in the temperature range 873 K (600 °C) to 1473 K (1200 °C) and strain rate range 0.001-100 s^{-1}, with the view to optimising the hot, warm and cold workability. The process parameters for the optimum workability in these materials are well documented. The microstructural studies conducted on stainless steel products formed at different temperatures and strain rates using industrial processing operations have confirmed that the predictions on the evolution microstructure based on laboratory tests.

A new methodology to refine the safe processing window for better microstructural control has been presented. It has been observed that the variance in grain size and mechanical

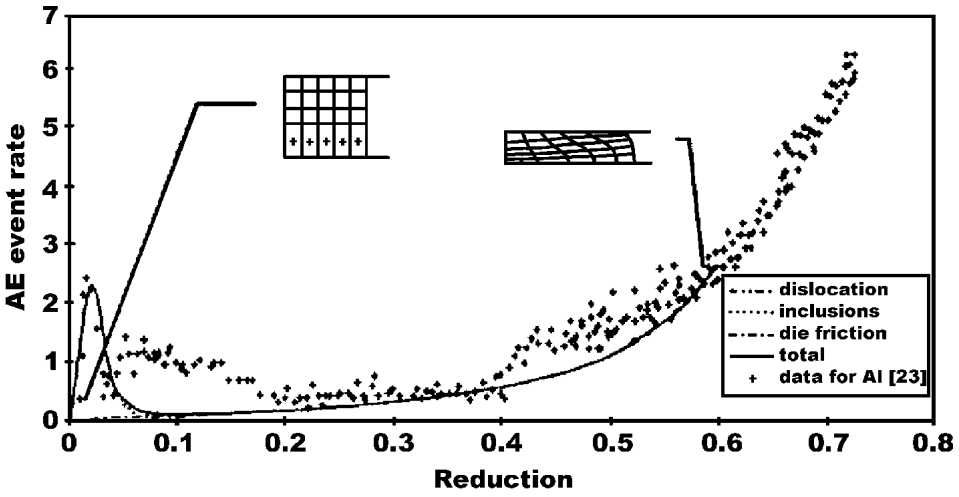

Fig. 12 AE during upsetting operation[36]

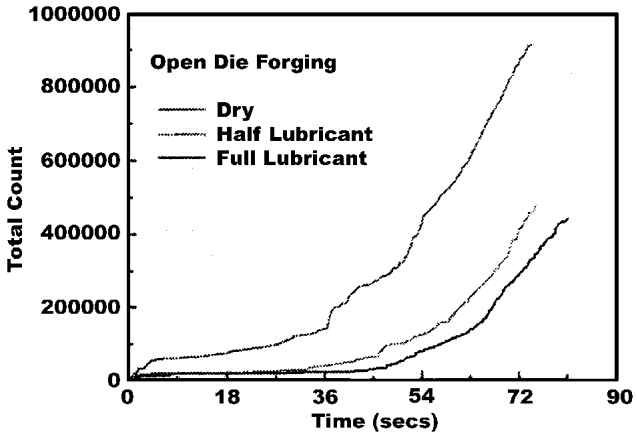

Fig. 13 AE at different friction conditions

properties of the products processed in stable domain is minimal. The validity of the proposed refining methodology for the design of deformation processes has been demonstrated with detailed forging and rolling trials at the industrial scale.

The two-stage methodology was utilized for optimal design of the hot extrusion process for stainless steel, type AISI 304L. In the first stage, equations for dynamic recrystallization of 304L were utilized to obtain an optimal deformation path, such that the grain size of the product would be 35 μm. In the second stage, the extrusion die profile has been developed such that the strain rate profile during extrusion matches with the optimal trajectory computed in the first stage. An extrusion experiment was performed to validate the proposed methodology by utilizing the extrusion die geometry obtained in the second stage. The as-extruded grain size was observed to be in close agreement with that for the optimal process design. These results have revealed that the principles of control theory could be reliably applied for the optimization and control of microstructure during industrial scale deformation processing.

Directions for future research in the areas of modeling shape

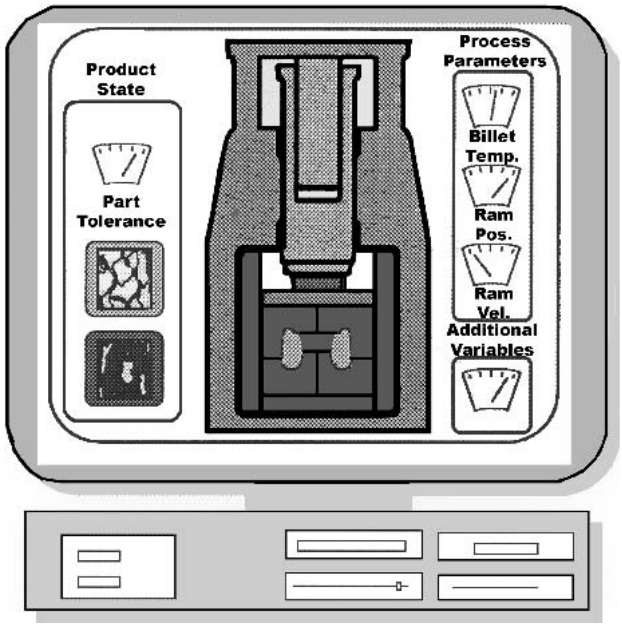

Fig. 14 Intelligent Forging System for monitoring and controlling the microstructure in the component during forging[37]

optimization and monitoring methods have been discussed. Methods for monitoring the process to attempt for on-line process control have also been discussed. The AE technique has proved to be a successful for assessing the lubricant condition and die filling. An intelligent system for the control of the process has been proposed.

References

1. N.J. Neale: *Tribology Handbook*, Butterworths, London, UK, 1983, p. 1.
2. D.T. Liewellyn and J.D. Murry: "Cold Worked Stainless Steels," Special Report 86, Iron and Steel Institute, London, 1964, 197.
3. D.T. Liewellyn and V.J. McNeely: "Metallurgical Development in High Alloy Steels," 1972, *49*(1) p. 17.

4. W. Shichun: "Warm Forging of Stainless Steels," *J. Mech. Technol*., 1982, *6,* p. 333.
5. S. Venkadesan: "Warm Working of Austenitic Stainless Steels," M.S. Thesis, IIT Madras, India, 1982.
6. W. Roberts: "Dynamic Changes that Occur During Hot Working and Their Significance Regarding Microstructural Development and Hot Workability" in *Deformation, Processing and Structure,* George Krauses, ed., ASM, Metals Park, OH, 1984, pp. 109-84.
7. M.C. Mataya, E.L. Brown, and M.P. Raendeau: "Effect of Hot Working on Structure and Strength of Type 304L Austenitic Stainless Steel," *Metall. Trans. A.*, 1990, *21A,* p. 1969.
8. S.K. Mehra, S.M. Rao, and N. Swaminathan: "Development of Thick Walled 304L Stainless Steel Seamless Tubes for Reactor Use," *Trans. Indian Inst. Metals*., 1987, *40*(1), p. 71.
9. S. Venugopal, M. Vasudevan, Sridhar Venugopal, P.V. Sivaprasad, S.K. Jha, P. Pandey, S.L. Mannan and Y.V.R.K. Prasad: "Industrial Validation of Processing Maps of Stainless Steel 304L Using Hot Rolling, Forging and Extrusion," *J. Mater. Sci. and Technol.,* 1996, *12,* pp. 955-62.
10. A.K. Gupta, K.E. Hughes, and C.M. Sellars: "Glass Lubricated Hot Extrusion of Stainless Steel," *Met. Technol*., 1980, *7,* p. 323.
11. K. Laue and H. Stenger: *Extrusion: Processes, Machinery, Tooling*, ASM, Metals Park, OH, 1981, p. 1.
12. S. Venugopal, S.L. Mannan, and Y.V.R.K. Prasad: "Influence of Strain-Rate and State-of-Stress on the Formation of Ferrite in Stainless Steel Type AISI 304 During Hot Working," *Materials Letters,* 1995, *26*, pp. 161-65.
13. F.B. Pickering: "Physical Metallurgy of Stainless Steel Developments," *Int. Met. Rev.,* Review No. 211, Dec. 1976, p. 227.
14. B. Ahlblom and R. Sandstrom: "Hot Workability of Stainless Steels: Influence of Deformation Parameters, Microstructural Components, and Restoration Processes," *Int. Met. Rev*., Review No. 1, 1982, p. 1.
15. M.C. Mataya and G. Krauss: "A Test to Evaluate Flow Localization During Forging," *J. Appl. Metal Working*, 1981, *2*(1), p. 28.
16. M.K. Malik: "Extrusion Principles and Applications to Steel" in P*roc. Intensive Course on Technology of Metal Forming,* ASM-Indian Chapter and IIM-Bombay Chapter, Bombay, Maharashtra, India, 26-28 Feb., 1982, p. 31.
17. C. Rossard and P. Blain: "Simulation by Torsion of Hot Rolling Conditions to Determine Their Influence on Steel," *Revue de Metallurgie,* 1965, *62,* pp. 881-90.
18. W.J. McG Tegart: "Ductility," ASM, Metals Park, Ohio, 1968, pp. 133-77.
19. H.J. McQueen and J.J. Jonas: "Recovery and Recrystallization During High Temperature Deformation" in *Treatise on Materials Science and Technology*, Vol. 6, Plastic Deformation of Materials, Academic Press Inc., New York, NY, 1975, pp. 394-493.
20. N.D. Ryan and H.J. McQueen: "Effects of Alloying Upon the Hot Workability of Carbon, Microalloyed, Tool, and Austenitic Stainless Steels" and "Mean Pass Flow Stresses and Interpass Softening in Multistage Processing of Carbon-, HLSA-, Tool- and -γ Stainless Steels," *J. Mech. Working Technol*., 1986, *12,* pp. 279-96 and 323-49.
21. C.M. Sellars: "Computer Modelling of Hot Working Processes," *Mater. Sci. Technol.*, 1985, *1,* p. 325.
22. H.L. Gegel, J.C. Malas, W.G. Frazier, and S. Venugopal: "Optimal Design of Thermomechanical Processes," in "Hand Book of Workability and Process Design," ed. G.E. Dieter, H.A. Kuhn and S.L. Semiatin, ASM, Materials Park, OH, 2003, pp. 337-45.
23. S. Venugopal and Baldev Raj: "A Holistic Approach to Thermomechanical Processing of Alloys," *Sadhana*, 2003, *28*, pp. 833-57.
24. Y.V.R.K. Prasad, H.L. Gegel, S.M. Doraivelu, J.C. Malas, J.T. Morgan, K.A. Lark, and D.R. Barker: "Modeling of Dynamic Material Behavior in Hot Deformation: Forging of Ti-6242," *Metall. Trans. A,* 1984, *15A,* p. 1883.
25. Kalyan Kumar: "Criteria for Predicting Metallurgical Instabilities in Processing," M.Sc., Thesis, Indian Institute of Science, Bangalore, India, 1987.
26. N.D. Ryan and H.J. McQueen: "Dynamic Softening Mechanisms in 304 Stainless Steels," *Can. Metall. Quarterly*, 1990, *29,* pp. 147-62.
27. S. Venugopal: "Optimization of Workability and Control of Microstructure in Deformation Processing of Austenitic Stainless Steels: Development and Application of Processing Maps for Stainless Steels Type AISI 304 and 316L," Ph.D. Thesis, University of Madras, India, 1993.
28. P.V. Sivaprasad, S.L. Mannan, Y.V.R.K. Prasad, and R.C. Chaturvedi: "Identification of Processing Parameters for Fe-15Cr-2.2Mo-15Ni-0.3Ti Austenitic Stainless Steel Using Processing Maps," *Mater. Sci. Technol.,* 2001, *17*, pp. 545-50.
29. S.L. Semiatin and G.D. Lagoti: "Deformation and Unstable Flow in Hot Forging of Ti-6A1-2Sn-4Zr-2Mo-0.1Si" and "Deformation and Unstable Flow in Hot Torsion of Ti-6Al-2Sn-4Zr-2Mo-0.1Si," *Metall. Trans. A*, 1981, *12A,* pp. 1705-17 and 1719-28.
30. P. Rodriguez: "Serrated Plastic Flow," *Bull. Mater. Sci.*, 1984, 6, pp. 653-63.
31. J.C. Malas and V. Seetharaman: "Using Materials Behavior Models to Develop Process Control Strategies," *J. Metals*, 1992, *44,* p. 8.
32. H.L. Gegel: private communication, 1998.
33. S. Venugopal, J.C. Malas, E.A. Medina, W.G. Frazier, S. Medeiros, W.M. Mullins, and R. Srinivasan: "Optimization of Microstructure During Deformation Processing Using Control Theory Principles," *Scripta Mater.*, 1997, *36,* pp. 347-53.
34. K.E. Kirk: *Optimal Control Theory*, Prentice-Hall, Englewood Cliffs, NJ, 1970, p. 1.
35. G.F. Vander Vooret: *Metallography, Principles and Practice*, ASM International, Metal Park, OH, 1989, p. 1.
36. W.M. Mullins, R.D. Irwin, J.C. Malas, and S. Venugopal: "Examination on the Use of Acoustic Emission for Monitoring Metal Forging Processes: A Study Using Simulation Technique," *Scripta Mater.,* 1997, *36,* pp. 967-74.
37. J.C. Malas: unpublished research, 1997.